PCCP

View Online
Dynamic Article Links

Cite this: *Phys. Chem. Chem. Phys.*, 2011, **13**, 6931–6935

www.rsc.org/pccp

PAPER

Unexpected optical response of single ZnO nanowires probed using controllable electrical contacts

Y. J. Zeng,*[a] M. Menghini,[a] D. Y. Li,[a] S. S. Lin,[b] Z. Z. Ye,[b] J. Hadermann,[c] T. Moorkens,[a] J. W. Seo,[d] J.-P. Locquet[a] and C. Van Haesendonck[a]

Received 4th January 2011, Accepted 11th February 2011
DOI: 10.1039/c1cp00012h

Relying on combined electron-beam lithography and lift-off methods Au/Ti bilayer electrical contacts were attached to individual ZnO nanowires (NWs) that were grown by a vapor phase deposition method. Reliable Schottky-type as well as ohmic contacts were obtained depending on whether or not an ion milling process was used. The response of the ZnO NWs to ultraviolet light was found to be sensitive to the type of contacts. The intrinsic electronic properties of the ZnO NWs were studied in a field-effect transistor configuration. The transfer characteristics, including gate threshold voltage, hysteresis and operational mode, were demonstrated to unexpectedly respond to visible light. The origin of this effect could be accounted for by the presence of point defects in the ZnO NWs.

Introduction

Since the pioneering experimental and theoretical reports on carbon nanotubes,[1–3] nanowires (NWs) have attracted world-wide attention due to the numerous unique properties that are expected for these one-dimensional anisotropic systems. In particular, semiconductor NWs have inspired numerous research efforts because of their tunable performance and wide-ranging device applications.[4] Zinc oxide (ZnO), by virtue of its excellent material properties, such as a wide direct bandgap of 3.37 eV at room temperature, a large exciton binding energy of 60 meV and the availability of high-quality bulk crystals, promises to be important for the next-generation electrical and opto-electronic devices.[5] On the other hand, ZnO NWs exhibit multifunctionality and have been configured as field-effect transistors (FETs),[6,7] piezoelectric nanogenerators,[8] gas sensors,[9] blue/ultraviolet (UV) light emitters,[10,11] and solar cells.[12,13] However, the electrical transport mechanism of single ZnO NWs, which is crucial for device applications, has not yet been fully understood.

The current–voltage (*I–V*) characteristics of as-fabricated semiconductor NWs can be either symmetric or asymmetric, depending in a very sensitive way on the type of contacts between the semiconductor NW and the metallic electrode.[14] If both contacts are ohmic, linear *I–V* curves are expected. On the other hand, rectifying *I–V* curves are predicted by thermionic emission theory when one of the contacts becomes Schottky type and the other contact remains ohmic. In the third case, *i.e.* when both contacts are Schottky type, one expects symmetric but non-linear *I–V* curves if the barrier height is equal for both contacts and asymmetric non-linear *I–V* curves otherwise. The *I–V* characteristics will be more complicated when the intrinsic resistance of the semiconductor NWs becomes comparable to or even higher than the contact resistance, which is very well possible due to the high length to diameter ratio of the NWs. Here, we demonstrate that the *I–V* characteristics of individual ZnO NWs can be varied between linear and asymmetric, depending on whether or not ion milling is used during the contact fabrication, which also results in a different UV light response.

Recently Wang introduced the so-called piezophototronic effect, a result of the three-way coupling between piezoelectricity, photonic excitations, and semiconductor electrical transport, which allows to tune and control electro-optical processes by a bending-induced piezopotential.[15] On the other hand, little attention has been paid to the electrical transport behavior of individual ZnO NWs under different illumination conditions. Here, we demonstrate that illumination, even with visible light of weak intensity, strongly affects the electrical transport through individual ZnO NW FETs.

Experimental

ZnO NW powders were grown in a horizontal furnace using a catalyst-free vapor phase deposition process. High purity Zn bulk metal was used as the Zn source and an O_2 flow was

[a] *Laboratory of Solid-State Physics and Magnetism, Katholieke Universiteit Leuven, Celestijnenlaan 200 D, BE-3001 Leuven, Belgium. E-mail: yujia.zeng@fys.kuleuven.be*
[b] *State Key Laboratory of Silicon Materials, Department of Materials Science and Engineering, Zhejiang University, Hangzhou 310027, P. R. China*
[c] *Electron Microscopy for Materials Science – EMAT, University of Antwerp, Groenenborgerlaan 171, BE-2020 Antwerp, Belgium*
[d] *Department of Metallurgy and Materials Engineering, Katholieke Universiteit Leuven, Kasteelpark Arenberg 44, BE-3001 Leuven, Belgium*

introduced acting as both the oxygen source and the carrying gas. The growth was maintained at a temperature of 700 °C and a pressure of 2200 Pa for 20 min. Next, the NW powders were dispersed in ethanol and transferred to heavily doped p-type silicon wafers with a top layer of 300 nm thermal oxide. The crystallographic orientation and microstructure of the ZnO NWs were characterized by X-ray diffraction (Philips PANalytical X'Pert PRO XRD system), electron diffraction (ED at Tecnai G2), high resolution high angle annular dark field scanning transmission electron microscopy (HRSTEM at Tecnai G2) and high resolution transmission electron microscopy (HRTEM at Tecnai G2). ZnO NWs were imaged by scanning electron microscopy (SEM at JEOL JSM-5600) and electrical contacts were attached to individual NWs by combining electron-beam lithography and lift-off techniques. *In situ* ion milling was used to remove possible contamination on the NW surface before deposition of 10 nm of Ti followed by 150 nm of Au. The electrical transport properties were investigated independently under different illumination conditions, including dark conditions, visible light of weak intensity, ambient light (5000–10 000 cd m^{-2}), and UV light. The FET transfer characteristics were measured (Keithley Model 4200-SCS) using the heavily doped Si substrates as the back gate electrode. A high power UV-LED (UV-Consulting Peschl portable lamp with wavelength of 365 nm) was used as a UV light source. The NW devices were kept in a home-made metallic box for one day before doing the measurements under dark conditions, in order to eliminate the presence of photo-induced carriers. Light-emitting diodes (LEDs) that generate different colors, *i.e.* red (623 nm, 1.8 cd), yellow (589 nm, 2.4 cd), green (525 nm, 2 cd), blue (470 nm, 0.9 cd) and white (3.5 cd), were installed inside the box, allowing illumination with color-selected light of weak intensity. All the *I–V* measurements with different illumination conditions were performed at room temperature around 20 °C and no special treatment of the atmosphere was used. Measurements were repeated a week and even one month later, the *I–V* characteristics were reproducible for each illumination condition, with typical results presented here.

Results and discussions

In Fig. 1 we present the XRD pattern of high density ZnO NWs lying on the Si/SiO_2 substrates. All diffraction peaks can be readily indexed and assigned to hexagonal-phase ZnO. No impurity phases can be detected in any of the XRD patterns. Apart from the most frequently observed (002) peak, also, *e.g.*, (100) and (101) peaks dominate the XRD pattern, which in our case is expected since the NWs lie flat and are randomly oriented on the substrates. The multiple peaks we observe are therefore not related to a polycrystalline nature of the ZnO NWs. We note that the NWs on the Si/SiO_2 substrates do not result in a complete coverage. The sharp diffraction patterns therefore suggest a good crystalline quality that is obtained by the vapor phase deposition.

Fig. 2 shows representative HRTEM (a) and HRSTEM (b) images of a single ZnO NW, as well as the corresponding ED pattern (c). A SEM image of an as-fabricated ZnO NW device is shown in Fig. 2d. The typical diameter of the NWs

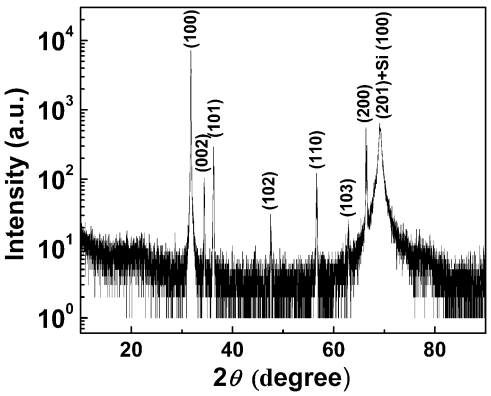

Fig. 1 XRD pattern of ZnO NWs deposited on Si/SiO_2 substrates.

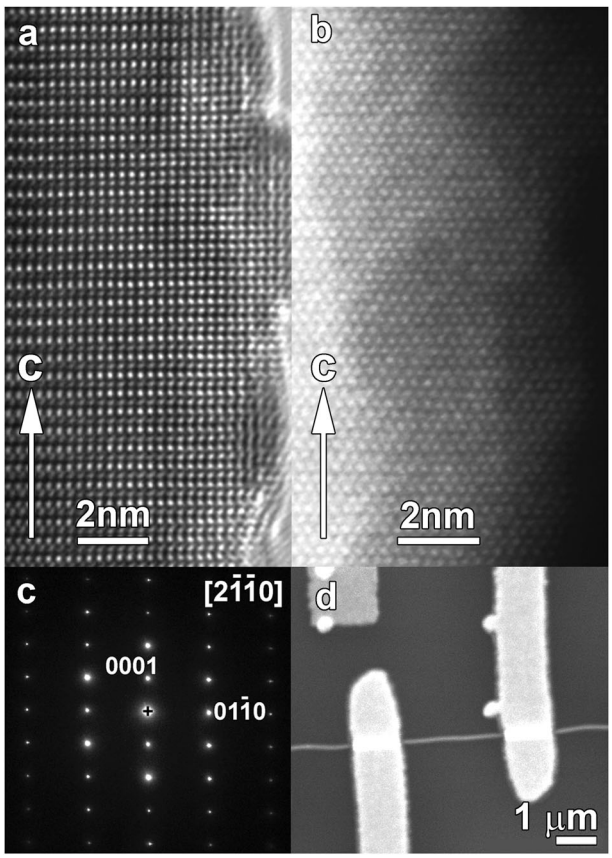

Fig. 2 (a) HRTEM image, (b) HRSTEM image, and (c) selected-area electron diffraction pattern of an individual ZnO NW, (d) SEM image of a ZnO NW device.

selected for attaching electrical contacts is around 100 nm. The TEM experiments reveal a single-crystalline nature for the ZnO NWs. The NWs grow along the [001] direction, *i.e.* the *c*-axis. The electron diffraction patterns can be indexed with the wurtzite structure using approximate cell parameters $a = 3.23$ Å, $c = 5.21$ Å (space group $P6_3mc$). Both HRTEM and HRSTEM images also correspond well with this structure. In the HRSTEM image the columns of Zn atoms are represented by the white dots over the whole area shown. In the more complex contrast of the HRTEM image there is only a direct

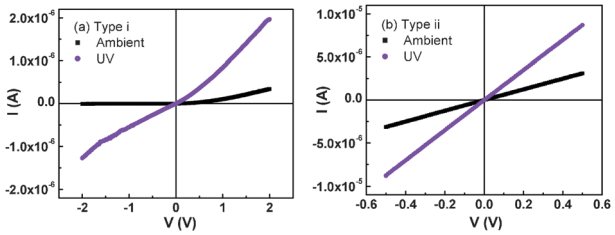

Fig. 3 *I–V* characteristics of (a) a type i and (b) a type ii ZnO NW under ambient light and UV light illumination.

interpretable visual relation in the thin area at the edge, where the columns of Zn atoms are represented by the black dots. Energy dispersive X-ray analysis performed during the TEM experiments does not reveal any presence of detectable impurities in the ZnO NWs (data not shown).

As mentioned in the Experimental section, *in situ* ion milling was used to remove possible contamination from the surface of the NWs before deposition of the metals for electrical contacts. In the following, the samples prepared without and with ion milling are referred to as type i and type ii NWs, respectively. In Fig. 3a we plot the *I–V* curve of a type i NW device under ambient light illumination, revealing a strongly asymmetric characteristic. At first glance, the curve appears to correspond to a Schottky diode behavior. However, according to more detailed data analysis (result not shown) the curve cannot be fitted using the well-known thermionic emission theory. We therefore believe that the type i NWs consist of back-to-back Schottky barriers, which is typically the case for semiconductor NWs.[14] The asymmetry indicates that the Schottky barrier height is different for the two contacts. Referring to Fig. 3a, the higher barrier is biased in the reverse direction when a negative voltage is applied and *vice versa*. When illuminated with UV light, the current flowing through the type i NWs increases dramatically. However, the *I–V* curve does not become completely symmetric, suggesting that different barriers are still present for the two contacts. The increase of the current can be assigned to a decrease of the Schottky barrier height and an increase of the carrier concentration, both effects resulting from the UV light illumination.

We now turn to the type ii NWs for which the ion milling process has been applied (see Fig. 3b). In contrast to the type i NWs, the type ii NWs carry large currents and have linear *I–V* curves, both under ambient light and UV light illumination. The linear *I–V* characteristics indicate the formation of ohmic contacts at both ends of the NW. Also, the ratio of the current change under UV illumination is considerably smaller than that for the type i NWs. This is not surprising because only the increase of carrier concentration contributes to the increase of the current for the type ii NWs.

The well-defined different types of electrical characteristics presented above are consistently observed for all investigated NWs. We therefore conclude that we are able to control the electrical contacts to the ZnO NWs by *in situ* ion milling. For the type i NWs, adsorbed oxygen[16] and/or possible contamination resulting from the electron-beam lithography process may give rise to the formation of a tunneling barrier and account for the observed Schottky type behavior. On the other hand, the *in situ* ion milling results in a clean surface of the NWs and allows to obtain a good ohmic contact between the ZnO and the Ti/Au electrode material. An alternative explanation for our experimental observations is that the contact properties can be associated with the piezoelectricity of the ZnO NWs. Strain may unintentionally be induced during material growth and/or the device fabrication process. As a result, a charge depletion zone can develop on the surface of the NWs, turning the contact into a Schottky barrier.[17] The ion milling process would then make the surface of the NWs amorphous or disordered to some extent, which reduces the strain and results in ohmic contact formation.

Next, we focus on the decay of the induced photocurrent after UV light illumination for the two types of electrical contacts. In Fig. 4a and b we present the photocurrent decay for the type i NWs. Referring to Fig. 3a, −2 V and +2 V correspond to the case when the higher Schottky barrier is biased in the reverse and forward directions, respectively. Both curves for the decay of the photocurrent can be nicely fitted using a stretched exponential function:

$$I = I_0 + (I_{uv} - I_0)\exp[-(t/\tau)^{\alpha}],$$

where I_0 and I_{uv} denote the "initial" current (before illumination) and the "peak" current ($t = 0$), respectively, τ is the time constant for the decay and α is the stretching exponent. In a similar way, we present in Fig. 4c the decay of the photocurrent for a type ii NW. The fitting parameters for both types of NWs are summarized in Table 1. The results listed in the

Table 1 The fitting parameters for the photocurrent decay after UV irradiation using a stretched exponential function

Sample	Type i (−2 V)	Type i (+2 V)	Type ii
I_{uv}/I_0	172.8	18.1	2.8
τ/s	14.8 ± 0.09	25.0 ± 0.08	4.5 ± 0.2
α	0.39 ± 0.001	0.48 ± 0.0009	0.45 ± 0.01

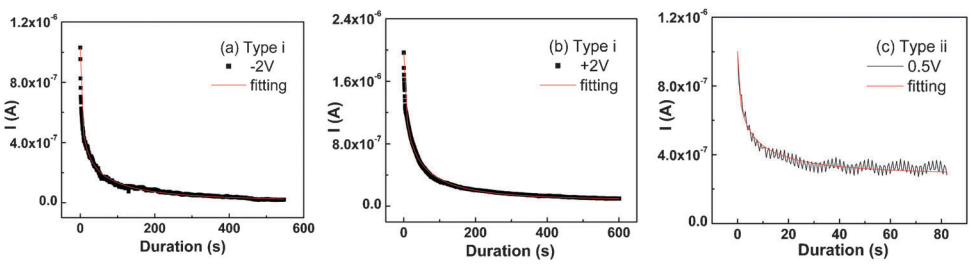

Fig. 4 Photocurrent decay after UV irradiation of a type i ZnO NWs when the higher Schottky barrier is biased in the reverse direction (a) and in the forward direction (b), and for a type ii ZnO NW (c). The red lines show the fitting curves using a stretched exponential function.

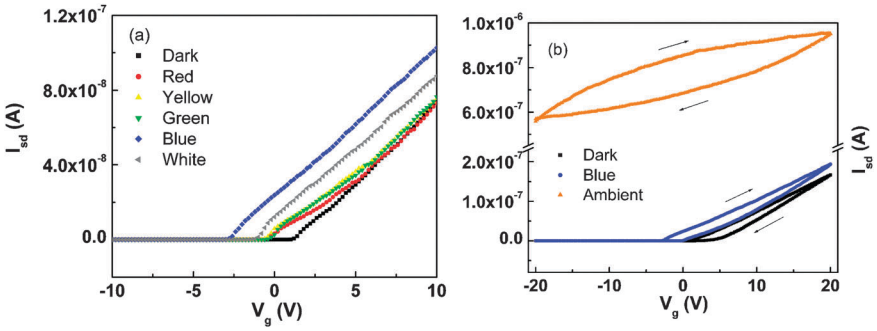

Fig. 5 (a) Source–drain current as a function of gate voltage in the dark and with LEDs illumination and a source–drain bias voltage of 100 mV. (b) Hysteretic behavior in the dark and under blue LED and ambient light illumination.

table indicate that the I_{uv}/I_0 ratio is much larger for the type i NWs, which can be understood in terms of the presence of the Schottky barriers. Moreover, when the higher barrier is reversed (−2 V), a higher ratio is observed due to the enhanced barrier height. On the other hand, it is clear that the time constant becomes much larger for the type i NWs, which can also be accounted for by the presence of the Schottky barrier. For the type i NWs, the decay behavior after UV irradiation involves restoration of the built-in electrical field resulting from the presence of the Schottky barriers as well as a decrease of the carrier concentration. When the higher barrier is biased in the reverse direction (−2 V), the restoration of the built-in electrical field is faster, implying a smaller time constant compared to that when the higher barrier is biased in the forward direction. This way, it is easy to understand the fast decay for the type ii NWs, where no Schottky barrier is involved in the electrical transport. However, the more noisy signals of type ii NWs may be due to the influence from ambient light illumination, which is present at the same time as the UV light illumination (see the discussion below).

For type ii NWs with good ohmic contacts, we also study their electrical transport characteristics in the FET configuration. Fig. 5a presents FET transfer characteristics for a ZnO NW in the dark and with LED light illumination using a source–drain bias voltage of 100 mV. We note that the intensity of the light produced by the LEDs is much weaker than the intensity of the ambient light that we use for illumination. The device reveals a typical n-type channel behavior, *i.e.*, the source–drain current increases with increasing positive gate voltage. The on–off ratios are about 10^4, indicating a good switching performance. Note that the leakage current through the gate and the drain is of the order of 10^{-12} A, which is considerably smaller than the source–drain current. The n-type conductivity of the ZnO can be ascribed to native defects and/or unintentional donor doping.[18–20] We would like to point out that the gate threshold voltage of the NW FETs shifts towards larger negative value with decreasing wavelength of the light. The decrease of the threshold voltage, in principle, indicates an increase of the carrier concentration in the channel at zero gate voltage. Therefore, the electrical properties of the ZnO NWs are not only sensitive to UV light illumination, as illustrated in Fig. 3b, but also respond to visible light with weak intensity.

In Fig. 5b, we compare the gate effects for measurements in the dark and for measurements under blue and ambient light illumination. Obviously, our NW FETs are in the enhancement mode (normally "off") in the dark. On the other hand, they change to a depletion-like mode (normally "on") under ambient light illumination, where the conductive channel cannot be switched off for voltages down to −20 V (maximum voltage for the instrument). The increase of source–drain current at zero gate voltage is up to 3 orders of magnitude under ambient light illumination. This phenomenon can be accounted for in terms of a dramatic increase of the carrier concentration due to the strong ambient light illumination. Another striking feature is the hysteresis that appears in the transfer characteristics and is even enhanced under ambient light illumination. Hysteresis has been observed in carbon nanotube based FETs and has been ascribed to the charge injection at the nanotube–dielectric interface.[21–23] As illustrated in Fig. 5b, after a sweep to positive V_g, the threshold voltage moves towards more positive values, suggesting injection of negative charges into the silicon oxide. Charge traps in the silicon oxide are probably populated by electrons injected from the NW channel, where the electric field is higher due to the cylindrical device geometry.[22] If the above-mentioned charge-injection model holds for our devices, it is not difficult to understand the enhanced hysteresis under ambient light illumination, where the carrier concentration in the channel increases and hence the charge injection is enhanced by the illumination. The change in the threshold voltage due to hysteresis can be as large as 2.6 V (see the illumination with blue light), which may allow the device to function as a nonvolatile memory cell.

Since the bandgap of ZnO is 3.37 eV at room temperature, corresponding to a wavelength of 368 nm, the observed response to visible light should be related to deep levels inside the bandgap.[24] Theoretically, ZnO typifies a class of materials that can be doped *via* native defects in only one way, *i.e.*, n-type doping.[25] In ZnO, a large oxygen-deficient non-stoichiometry can be present regardless of the growth conditions.[26] Also, electron photoconductivity in n-type ZnO caused by the presence of oxygen vacancies has been predicted.[27] More recently, it has been demonstrated that ZnO NW FETs show a markedly different performance depending on whether oxygen-rich or oxygen-poor conditions were used for the NW growth.[28] We therefore believe that the native defects, such as oxygen vacancies or zinc interstitials, account for the observed response to visible light. In addition, there exist

many surface states for ZnO NWs due to the large surface to volume ratio. These surface states could drive the donor levels deeper in the bandgap, making them neutral in the dark and ionized under the visible light illumination. The ionization rate depends on both the wavelength and the intensity of the illumination. This fact might account for the large visible light response of ZnO NWs, which is not typically observed in ZnO bulk or thin films. More experimental as well as theoretical work is needed to better understand the exact origin of this behavior.

Conclusions

In conclusion, we presented a straightforward method to control the properties of the electrical contacts that are attached to individual ZnO NWs. The switch between Schottky and ohmic type of the contacts can be explained by the presence of residual contamination and/or strain near the NW surface. We found that the response of the ZnO NWs to UV irradiation can be controlled as well by the type of contact. Finally, we demonstrated that the transfer characteristics of individual ZnO NW FETs, including the gate threshold voltage, hysteresis and even the operational mode, respond to visible light illumination, strongly depending on both the wavelength and the intensity. The origin of this response may be ascribed to the presence of point defects in the ZnO, but clearly requires further investigation. Nevertheless, the observed effects are of fundamental importance for the electrical performance of ZnO NWs and need to be taken into account when designing ZnO NW based devices.

Acknowledgements

The work has been supported by the Research Foundation-Flanders (FWO, Belgium), by the Belgian Interuniversity Attraction Poles research program (IAP P6/42), and by the K. U. Leuven through the Concerted Research Action program (GOA/09/006) and the Centers of Excellence program (INPAC, Grant No. EF/05/005). The work at Zhejiang University was supported by the National Basic Research Program of China under Grant No. 2006CB604906.

References

1 S. Iijima, *Nature*, 1991, **354**, 56.
2 J. W. Mintmire, B. I. Dunlap and C. T. White, *Phys. Rev. Lett.*, 1992, **68**, 631.
3 N. Hamada, S. Sawada and A. Atsushi Oshiyama, *Phys. Rev. Lett.*, 1992, **68**, 1579.
4 Y. N. Xia, P. D. Yang, Y. G. Sun, Y. Y. Wu, B. Mayers, B. Gates, Y. D. Yin, F. Kim and Y. Q. Yan, *Adv. Mater.*, 2003, **15**, 353.
5 Ü. Özgür, Y. I. Alivov, C. Liu, A. Teke, M. A. Reshchikov, S. Doğan, V. Avrutin, S. J. Cho and H. Morkocd, *J. Appl. Phys.*, 2005, **98**, 041301.
6 Y. W. Heo, D. P. Norton, L. C. Tien, Y. Kwon, B. S. Kang, F. Ren, S. J. Pearton and J. R. LaRoche, *Mater. Sci. Eng., R*, 2004, **47**, 1.
7 P. C. Chang and J. G. Lu, *IEEE Trans. Electron Devices*, 2008, **55**, 2977.
8 Z. L. Wang and J. H. Song, *Science*, 2006, **312**, 242.
9 L. Liao, H. B. Lu, J. C. Li, H. He, D. F. Wang, D. J. Fu and C. Liu, *J. Phys. Chem. C*, 2007, **111**, 1900.
10 M. H. Huang, S. Mao, H. Feick, H. Q. Yan, Y. Y. Wu, H. Kind, E. Weber, R. Russo and P. D. Yang, *Science*, 2001, **292**, 1897.
11 J. M. Bao, M. A. Zimmler, F. Capasso, X. W. Wang and Z. F. Ren, *Nano Lett.*, 2006, **6**, 1719.
12 C. Levy-Clement, R. Tena-Zaera, M. A. Ryan, A. Katty and G. Hodes, *Adv. Mater.*, 2005, **17**, 1512.
13 K. S. Leschkies, R. Divakar, J. Basu, E. Enache-Pommer, J. E. Boercker, C. B. Carter, U. R. Kortshagen, D. J. Norris and E. S. Aydil, *Nano Lett.*, 2007, **7**, 1793.
14 Z. Y. Zhang, K. Yao, Y. Liu, C. H. Jin, X. L. Liang, Q. Chen and L. M. Peng, *Adv. Funct. Mater.*, 2007, **17**, 2478.
15 Z. L. Wang, *J. Phys. Chem. Lett.*, 2010, **1**, 1388.
16 Y. J. Zeng, Z. Z. Ye, Y. F. Lu, J. G. Lu, W. Z. Xu, L. P. Zhu, B. H. Zhao and Y. Che, *Chem. Phys. Lett.*, 2007, **441**, 115.
17 X. D. Wang, J. Zhou, J. H. Song, J. Liu, N. S. Xu and Z. L. Wang, *Nano Lett.*, 2006, **6**, 2768.
18 A. F. Kohan, G. Ceder, D. Morgan and C. G. Van de Walle, *Phys. Rev. B: Condens. Matter*, 2000, **61**, 15019.
19 C. G. Van de Walle, *Phys. Rev. Lett.*, 2000, **85**, 1012.
20 S. F. J. Cox, E. A. Davis, S. P. Cottrell, P. J. C. King, J. S. Lord, J. M. Gil, H. V. Alberto, R. C. Vilao, J. Piroto Duarte, N. Ayres de Campos, A. Weidinger, R. L. Lichti and S. J. C. Irvine, *Phys. Rev. Lett.*, 2001, **86**, 2601.
21 M. S. Fuhrer, B. M. Kim, T. Dürkop and T. Brintlinger, *Nano Lett.*, 2002, **2**, 755.
22 M. Radosavljevic, M. Freitag, K. V. Thadani and A. T. Johnson, *Nano Lett.*, 2002, **2**, 761.
23 Y. G. He, H. G. Ong, Y. Zhao, S. L. He, L. J. Li and J. L. Wang, *J. Phys. Chem. C*, 2009, **113**, 15476.
24 Y. Y. Tay, T. T. Tan, F. Boey, M. H. Liang, J. Ye, Y. Zhao, T. Norby and S. Li, *Phys. Chem. Chem. Phys.*, 2010, **12**, 2373.
25 S. B. Zhang, S. H. Wei and A. Zunger, *Phys. Rev. B: Condens. Matter*, 2001, **63**, 075205.
26 J. H. W. De Wit, *J. Solid State Chem.*, 1975, **13**, 192.
27 S. Lany and A. Zunger, *Phys. Rev. B: Condens. Matter*, 2005, **72**, 035215.
28 D. S. Kim, J.-P. Richters, R. Scholz, T. Voss and M. Zacharias, *Appl. Phys. Lett.*, 2010, **96**, 123110.